

CIRCUS: Circuit Consensus under Uncertainty via Stability Ensembles

Swapnil Parekh
Intuit

Abstract

Mechanistic circuit discovery is notoriously sensitive to arbitrary analyst choices, especially pruning thresholds and feature dictionaries, often yielding brittle “one-shot” explanations with no principled notion of uncertainty. We reframe circuit discovery as an uncertainty-quantification problem over these analytic degrees of freedom. Our method, CIRCUS, constructs an ensemble of attribution graphs by pruning a single raw attribution run under multiple configurations, assigns each edge a stability score (the fraction of configurations that retain it), and extracts a strict-consensus circuit consisting only of edges that appear in all views. This produces a threshold-robust “core” circuit while explicitly surfacing contingent alternatives and enabling rejection of low-agreement structure. CIRCUS requires no retraining and adds negligible overhead, since it aggregates structure across already-computed pruned graphs. On Gemma-2-2B and Llama-3.2-1B, strict consensus circuits are $\sim 40\times$ smaller than the union of all configurations while retaining comparable influence-flow explanatory power, and they outperform a same-edge-budget baseline (union pruned to match the consensus size). We further validate causal relevance with activation patching, where consensus-identified nodes consistently beat matched non-consensus controls ($p = 0.0004$). Overall, CIRCUS provides a practical, uncertainty-aware framework for reporting trustworthy, auditable mechanistic circuits with an explicit core/contingent/noise decomposition.

1 Introduction

Identifying *circuits*—sparse subgraphs of a model’s computation that causally support a behavior—is a central goal of mechanistic interpretability. Modern pipelines replace MLP layers with interpretable feature models (e.g., cross-layer transcoders) and build *attribution graphs* whose nodes are features, errors, tokens, and logits, and whose edges encode direct effects [Ameisen et al., 2025, Lindsey et al., 2025]. Pruning then retains edges that explain a large fraction of the output, yielding a compact circuit. A critical but often unstated issue is **uncertainty**: the resulting circuit depends on the choice of pruning thresholds and on which feature dictionary (e.g., which transcoder checkpoint) is used. Different choices yield different edges and different interpretations, with no principled way to separate stable structure from artifacts. We ask: can we leverage this variability to identify which circuit structure is stable and which is artifact?

We propose to treat circuit discovery as an *uncertainty quantification* problem. Rather than reporting a single graph, we (i) generate multiple graphs by varying pruning configurations; (ii) assign each edge a *stability score* as the fraction of views that retain it; and (iii) define a *consensus* subgraph—edges appearing in all views—as the threshold-robust circuit (Section 3.3). This **bagged attribution** pipeline quantifies which parts of the circuit are stable and which are uncertain. We aggregate *structure* (which edges appear), not saliency scores [Paillard et al., 2026], and expose a rejection/alternatives interface. Figure 1 illustrates the pipeline (Section 3). Empirically, con-

sensus retains at least as much explanatory power as some single-config graph in all 20 prompts and extends to multi-prompt stability and boosting.

Contributions. Method: We introduce a bagged-circuit pipeline that (i) samples a set of pruning configurations, (ii) assigns each edge a frequency-based **stability** score, (iii) extracts a strict-consensus circuit C_τ with an explicit rejection/alternatives interface, and (iv) supports stability–influence ranking plus tiered boosting (core vs. residual vs. full). **Empirics:** On Gemma-2-2B and Llama-3.2-1B Gemma Team et al. [2024], Meta AI et al. [2024], strict consensus is $\sim 40\times$ smaller than a loose prune at similar influence retained, outperforms a same-budget union-pruned baseline, and satisfies prompt-level sanity and compactness checks; we report bootstrap confidence intervals for stability and size–retained trade-offs. **Validation & diagnostics:** We complement within-method metrics with causal tests (activation patching) and diagnostics for multi-prompt stability and view diversity (e.g., Jaccard overlap), yielding a practical uncertainty-aware “core/contingent/noise” circuit taxonomy.

2 Related Work

Mechanistic interpretability. Mechanistic interpretability aims to reverse-engineer the internal computations of neural networks into human-understandable mechanisms [Olah, 2022]. Recent surveys organize the field around features (interpretable directions in activations), circuits (sparse subgraphs that implement behaviors), and methods for localization and causal intervention [Rai et al., 2024, Sharkey et al., 2025]. Evaluation frameworks for interpretability emphasize application-grounded, human-grounded, and functionally-grounded metrics [Doshi-Velez and Kim, 2017]. A central technique for testing causal importance of components is *activation patching* (causal tracing / interchange intervention), for which methodological choices—e.g., evaluation metrics and corruption methods—strongly affect which components are deemed important; Zhang and Nanda [2024] systematize best practices. Our work operates within this pipeline: we take attribution-

based circuit discovery as given and address *uncertainty* in the resulting graph structure when analyst choices (thresholds, dictionaries) vary.

Circuit tracing and attribution graphs. Ameisen et al. [2025] and Lindsey et al. [2025] introduce replacement models that substitute MLP layers with cross-layer transcoders (CLTs), enabling attribution graphs over interpretable features. The circuit-tracer library [Hanna et al., 2025] implements this for Gemma-2-2B and Llama-3.2-1B [Gemma Team et al., 2024, Meta AI et al., 2024] with public CLTs. Attribution circuits vary with pruning thresholds and with the choice of transcoder; a single run is thus one of many plausible explanations. Pruning is done by cumulative influence thresholds; the resulting graph is a single point estimate with no notion of stability across configs. Prior interpretability work by Parekh et al. [2020] and Kumar et al. [2023] studies which features (e.g., coherence, content) automated scoring models rely on and why they are susceptible to adversarial samples, with the latter proposing defenses based on attribution patterns; Singla et al. [2022] mine universal adversarial triggers for NLP models in a data-free setting. Our bagged pipeline addresses threshold and dictionary uncertainty in graph-based circuit discovery directly.

Ensembling and aggregation. Gadgil et al. [2025] apply bagging and boosting to sparse autoencoders, improving reconstruction and stability; Gyawali et al. [2022] show that ensembling feature importance across models and epochs improves stability and power of feature selection in deep learning. Paillard et al. [2026] caution that aggregating explanations post hoc can be lossy. We aggregate *which edges* appear (structure) with a clear agreement semantics and report the trade-off between consensus size and influence retained explicitly; our method is compatible with any attribution pipeline that produces multiple pruned graphs.

Faithfulness. We use *influence retained* (IR) as a within-method proxy [Ameisen et al., 2025] and activation patching [Zhang and Nanda, 2024] for causal validation; full faithfulness via replacement-model masking remains future work.

Uncertainty in circuits and explanations. Recent work studies uncertainty in transformer cir-

cuts via single-pass, white-box scores (e.g., coherence of one circuit [Krasnovsky, 2025]); other work explains predictive uncertainty via second-order attribution effects [Bley et al., 2024] or quantifies stability of attribution-based explanations under input or model changes [Agarwal et al., 2022]. We instead quantify uncertainty by *agreement across multiple views*, yielding a direct stability score per edge. We focus on uncertainty over *explanation structure*—which edges to trust when analyst choices vary—not predictive uncertainty of the model. We compare against a *single fixed-threshold circuit* and the *union of all threshold configs*; we report strict consensus ($\tau = 1$) and can use $\tau = 2/3$ for a larger exploratory set. Our stability score can be used as an epistemic rejection criterion for unreliable circuit edges [Zhu et al., 2025].

3 Methodology

3.1 Notation and Problem Formulation

We formalize the setting. Let $\mathcal{G} = (V, E, W)$ denote the *full attribution graph* for a fixed prompt and target token: V is the set of nodes (features, errors, tokens, logits), E the set of directed edges, and $W \in \mathbb{R}^{|E|}$ the edge weights (direct effects). The full graph is produced by a replacement model (CLT) and is typically large. A *pruning configuration* π (e.g., node and edge cumulative-influence thresholds) yields a *pruned graph* with edge set $E^{(\pi)} \subseteq E$. We treat multiple configurations as B *views* (one view = one pruned graph per configuration); the b -th view has edge set $E^{(b)} \subseteq E$.

Edge stability. For each edge $e \in E$, the *stability score* $s(e)$ is the fraction of views that retain it; it reflects agreement across analyst choices, not causal correctness.

$$s(e) = \frac{1}{B} \sum_{b=1}^B \mathbb{1}[e \in E^{(b)}]. \quad (1)$$

So $s(e) \in [0, 1]$; $s(e) = 1$ iff e appears in all views.

Consensus and union. For a threshold $\tau \in [0, 1]$,

the *consensus subgraph* is the set of edges with stability at least τ :

$$C_\tau = \{e : s(e) \geq \tau\}. \quad (2)$$

We use $\tau = 1$ for the strict consensus (edges in every view) and can use $\tau = 2/3$ for a larger exploratory set. Unlike classic stability selection, we do not choose τ by formal FDR control; we use the IR-size trade-off (or a fixed edge budget) and report the elbow curve (Figure 3). **Default:** show strict consensus ($\tau = 1$); if the user wants alternatives, show influential low-stability edges. The *union* is $E^{\text{union}} = \bigcup_{b=1}^B E^{(b)}$ (all edges that appear in at least one view).

Influence retained. For a subgraph with edge set $S \subseteq E$, let $\Phi(S)$ denote the total influence from nodes to the output logits when only edges in S are retained. Following Ameisen et al. [2025], $\Phi(S)$ is computed via the row-normalized adjacency of the subgraph induced by S , with power iteration to the output logits. We define

$$\text{IR}(S) = \frac{\Phi(S)}{\Phi(E)}. \quad (3)$$

So $\text{IR}(S) \in [0, 1]$ is the fraction of total graph influence flowing through S ; we use it for within-method comparison only. For the *residual* subgraph (edges not in C_1), connectivity differs and the ratio to $\Phi(E)$ can exceed 1; we report that value separately as **residual flow** when needed. **Consensus checks** (reported in Results): (i) *Sanity check:* $\text{IR}(C_\tau) \geq \min_{b \in [B]} \text{IR}(E^{(b)})$. (ii) *Pareto compactness:* consensus achieves $\text{IR}(C_\tau) \geq (1 - \varepsilon) \max_b \text{IR}(E^{(b)})$ (e.g., $\varepsilon = 16.3\%$) while using at most a small fraction of the edges of the best single config (e.g., 2.5%). We also compare to **union pruned to $|C_1|$** : take the union of all views, then keep the top $|C_1|$ edges by influence (same edge budget as consensus).

Problem. Given B views with edge sets $\{E^{(b)}\}_{b=1}^B$, we wish to (i) assign each edge a stability score $s(e)$; (ii) report a threshold-robust consensus C_τ ; and (iii) refine with a second round (boosting) on the residual influence when desired. Figure 1 summarizes the pipeline; the following subsections and algorithms detail the procedure.

Pipeline overview.

- **Inputs:** Raw attribution graph \mathcal{G} ; B pruning configurations (threshold grid or design set).
- **Outputs:** Per-edge stability $s(e)$ (Eq. 1); consensus subgraph C_τ (Eq. 2); boosted circuit $C_1 \cup C_2$ when desired (Section 3.4).
- **Key parameter:** $\tau \in [0, 1]$ trades circuit size vs. influence retained; default $\tau = 1$ (strict consensus).
- **Outputs and metrics:** Core circuit $C_{\tau=1}$; exploratory circuit C_τ for $\tau < 1$ plus high-influence, low-stability alternatives; boosted $C_1 \cup C_2$ for residual coverage. Metrics: $|C_\tau|$, $\text{IR}(C_\tau)$ [Ameisen et al., 2025], stability distribution, view diversity (e.g., Jaccard).

See Section 3.1 for notation and Appendix D for algorithmic steps.

3.2 Attribution Graphs and Pruning

We assume a *replacement model*: the base LM’s MLPs are replaced by a cross-layer transcoder (CLT) that approximates MLP outputs with sparse features. For a fixed prompt and target token, the *attribution graph* has nodes for active features (layer, position), error nodes, input tokens, and output logits; edges encode direct linear effects. The full graph is large; *pruning* keeps nodes/edges that explain a fraction (e.g., 98%) of cumulative influence to the logits, yielding a sparse circuit. Different node and edge cumulative-influence thresholds produce different pruned graphs from the same raw attribution.

3.3 Config-Bagging and Uncertainty Decomposition

We address epistemic uncertainty regarding analyst choices by treating plausible pruning thresholds as a finite design set. Rather than resampling data, we use **parameter-space bagging** (config-bagging): one attribution run, then B pruning configurations

Table 1: Uncertainty decomposition: two sources of variability.

Type	Source	Definition
Epistemic (analytic)	Var. by π	Edge stability $s(e)$ over threshold/dictionary design set; low agreement \Rightarrow sensitive to analyst choices.
Instance (aleatoric-like)	Var. by prompt	Variance of IR and edge sets across prompts (Section 5.3); some prompts admit a stable circuit.

yield B views, each a subset of edges from the same full graph. No new model training is required.

This approach allows us to decompose circuit uncertainty into two primary sources (Table 1).

Epistemic (analytic) uncertainty: Variance driven by the choice of threshold or dictionary. We quantify this via an edge’s stability score $s(e)$ (Eq. 1). Under a threshold-sweep, the fraction of single-config graphs that retain a specific edge equals its selection probability over the design set [Meinshausen and Bühlmann, 2010]. This **frequency semantics** directly measures an edge’s robustness to analyst choices.

Instance (aleatoric-like) variability: Variance across different prompts, reported via multi-prompt variance and worst-case influence retained (IR) (Section 5.3).

Using this framework, we establish a practical **circuit taxonomy**. Edges with $s(e) = 1$ form the *core* consensus circuit C_1 . Edges with medium stability but high marginal influence are *contingent* (alternative pathways); low-stability, low-influence edges are *noise* and can be rejected (e.g., flag edges with $s(e) < \tau_{\text{rej}}$ such as 0.5). Stability measures agreement across configurations, not causal correctness. We validate causal relevance via activation patching (Section 5.4); replacement-model masking remains future

work. Appendix D gives the full procedure.

3.4 Boosting: Residual Uncertainty Test

The *core* consensus circuit C_1 (Section 3.1) is the strict-consensus subgraph. Boosting is a **residual uncertainty test**: if C_1 has low IR, the *boosted* circuit C_2 (built from the residual graph) reveals where *contingent* or *missing* influence lives. After C_1 , we build a *residual graph* by zeroing C_1 edges in the adjacency matrix and compute per-edge influence on this graph; C_2 contains edges with highest residual influence (e.g., top 90%). The **boosted** circuit is $C_1 \cup C_2$. We report IR [Ameisen et al., 2025] for C_1 , C_2 , and $C_1 \cup C_2$, and a *compact* variant and a *post-pruned* circuit. Appendix D gives the full procedure.

4 Experiment Design

Models and data. We fix the attribution; the only variation is analyst choices. Any randomness (e.g., bootstrap over configs, corruption-slot sampling in activation patching [Zhang and Nanda, 2024]) is made explicit. We use Gemma-2-2B and Llama-3.2-1B [Gemma Team et al., 2024, Meta AI et al., 2024] with publicly available cross-layer transcoders [Ameisen et al., 2025, Hanna et al., 2025]. Prompts are short completions: one fixed prompt for threshold-sweep, 20 prompts for multi-prompt and intervention analyses. The prompt set includes factoid completions (capitals, arithmetic, trivia) chosen to vary difficulty and length; see supplement for full list. Results are on 1B–2B parameter models and short completions; generalization to larger models or long-form tasks is future work.

Threshold-sweep. One attribution run; we report both $B = 3$ (minimal: configs (0.6, 0.95), (0.8, 0.98), (0.9, 0.99)) and $B = 25$ (5×5 node/edge threshold grid over the same range) as primary settings. The $B = 25$ grid is explicitly: node thresholds in $\{0.6, 0.7, 0.8, 0.9, 0.95\}$ and edge thresholds in $\{0.95, 0.96, 0.97, 0.98, 0.99\}$ (see supplement for full enumeration). With $B \gg 3$, stability is no longer tri-level; we report stability histograms, consensus size

and IR vs. τ , and bootstrap 95% CIs over configs for $|C_1|$ and $\text{IR}(C_1)$. We compute edge/node stability and consensus ($\tau = 1$). Baselines: single fixed-threshold (each config), union (all edges in ≥ 1 config), consensus, and **union pruned to $|C_1|$** (same edge budget as consensus). We report IR for each and the two consensus checks (sanity check and Pareto compactness). We also report config-drop (leave-one-config-out), stability–influence correlation, **approximate intervention** (graph-level ablation; pre-registered Spearman), **robustness** (worst-case / std of IR across prompts), **stability-weighted selection** (consensus vs. top- k by influence at fixed k), **circuit taxonomy** (core / contingent / noise), and **view diversity** (pairwise Jaccard between configs).

Multi-prompt. Same pipeline over 20 prompts for multi-prompt and intervention analyses; one model load, one attribution per prompt. We also report 5-prompt worst-case IR where noted. We report mean and variance of IR across prompts for each config and consensus (stability), and single-run baseline vs. consensus.

Boosting. After the threshold-sweep we take consensus as C_1 , build C_2 from residual influence (top 90% of residual), and report tiered results: core (C_1), residual (C_2), full ($C_1 \cup C_2$), compact full, and post-pruned (95% influence). **Efficiency:** Building consensus or union from prune results adds negligible cost (order of milliseconds) compared to a single influence-retained computation (~ 10 ms in our setup).

Activation patching and ablation. For causal validation we use activation patching on the base LM: we zero a random 50% of (layer, position) slots, then patch back k slots from the clean run and measure recovery = patched logit – corrupted logit for the clean target token. The *matched* baseline uses the same k slots and layer/position-type distribution sampled from *non-consensus* slots so the control is not confounded by structure. We also report ablation (zero residual stream at consensus positions) with the same matched baseline. Details and sanity checks are in Section 5.4.

Table 2: Influence retained for single-config and consensus (representative run, $B = 3$ configs). Row labels refer to threshold values: looser thresholds (0.9, 0.99) retain more edges; stricter (0.6, 0.95) yield a smaller graph.

Graph	Edges	IR
Loose (0.6, 0.95)	625	0.78
Mid (0.8, 0.98)	6,917	0.88
Strict (0.9, 0.99)	25,478	0.93
Union (≥ 1 config)	25,478	0.93
Consensus ($\tau = 1$)	625	0.78
Union pruned to $ C_1 $	625	0.73

5 Results

5.1 Threshold-Sweep and Consensus

Key result: Consensus is $\sim 40\times$ smaller than the union at similar IR, outperforms the same-edge-budget baseline (union pruned to $|C_1|$), and passes the sanity check in 20/20 prompts.

From a single attribution run with three pruning configs ($B = 3$), we obtain edge and node stability and a consensus subgraph. We compare *single fixed-threshold* graphs (loose, mid, and strict threshold sets), the *union* of all configs (edges present in ≥ 1 config), and *consensus* ($\tau = 1$). Table 2 summarizes this run: the union has 25,478 edges; consensus has 625 (a $\sim 40\times$ reduction) with IR 0.78. The same-budget comparison—union pruned to $|C_1|$ edges—gives IR 0.73 vs. consensus 0.78, so threshold-robust selection beats this baseline. The sanity check holds in 20/20 prompts (Section 5.3). **Pareto compactness** holds: consensus achieves IR within 16.3% of the best single threshold set while using 2.5% of its edges (Table 2). Stability distribution shows many edges appear in only one or two configs, underscoring threshold uncertainty. See Appendix B for IR vs. edge budget and Figure 6.

With $B = 25$ configs we obtain a rich stability distribution and bootstrap CIs (Figure 3). **Stability–influence:** Mean per-edge influence increases with stability: edges in all three configs have $\sim 70\times$ higher mean influence than edges in one config (same run),

supporting that high-stability edges are both stable and consequential (Figure 5).

Causal validation (activation patching). We validate via activation patching [Zhang and Nanda, 2024, Wang et al., 2024]. Consensus nodes mapped to (layer, position) consistently outperform matched baselines when patching back into a corrupted run ($p = 0.0004$; see Section 5.4 for experimental details). Figure 2 shows the per-prompt recovery difference (consensus – control and consensus – matched), giving strong evidence for the claim that consensus edges matter.

Figure 3 shows the trade-off between consensus threshold τ , circuit size, and IR: as τ increases, $|C_\tau|$ drops while IR remains relatively high until strict consensus. With $B = 25$ configs the stability distribution is rich (Section 5.4); bootstrap 95% CIs over configs are shown at $\tau = 1$. **Config-drop** (leave-one-config-out): dropping the loosest config changes consensus substantially, while dropping a stricter config does not (Figure 4), so the consensus is not driven by a single strict configuration.

5.2 Boosting: Core, Residual, and Full

Boosting: core, residual, and full. The *core* consensus C_1 is a compact, threshold-robust circuit (625 edges, 61 nodes, IR 0.78 in this $B = 3$ run) suitable for interpretation and auditing. Boosting is a **diagnostic for residual importance**—how much influence flows outside C_1 —and recovers coverage. Table 3 reports tiered boosting. C_2 adds edges that carry influence not flowing through C_1 ; the full circuit $C_1 \cup C_2$ achieves IR 0.96 but is large (36,350 edges). A *compact* variant uses 9,546 edges with IR 0.91; post-pruning the full circuit to 95% influence yields 18,690 edges and IR 0.94. When C_2 is very large, the full circuit undermines interpretability; the compact or post-pruned variant then gives a better size–coverage trade-off.

Table 3: Tiered Boosting: Core, Residual, Full, and Variants.

Circuit	Edges	Nodes	IR
C_1 (core)	625	61	0.78
C_2 (residual)	35,725	1,183	—
$C_1 \cup C_2$ (full)	36,350	1,184	0.96
$C_1 \cup C_2$ compact	9,546	942	0.91
Post-pruned (95%)	18,690	1,045	0.94

Note: IR is defined only for subgraphs of the full graph with the same reference $\Phi(E)$, so it lies in $[0, 1]$.

Residual C_2 alone is computed on a different (residual) graph; we report *residual flow* there (omitted) and full/post-pruned IR for interpretable comparisons.

5.3 Multi-Prompt and Single-Baseline Trade-off

Our multi-prompt set includes factoid completions (capitals, arithmetic, trivia) and reasoning-style prompts to check robustness across task types. Over 20 prompts, the sanity check held in 20/20 in this run; mean consensus influence retained (IR) was 0.83 ± 0.05 . Consensus size ranges from 625 to 1,288 edges across prompts (e.g., “The capital of France is” 625; “The largest planet in the solar system is” 1,288). Consensus mean IR can be slightly lower than a single mid-threshold baseline; we report this explicitly: consensus trades some IR for *threshold robustness* and interpretability (edges in all configs). When threshold choice is uncertain, consensus is a principled default.

5.4 Uncertainty Analyses: Rejection, Alternatives, Variance

Rejection criterion. On a representative run (25,478 edges in ≥ 1 config), 2.5% have stability = 1 (625 edges, strict consensus) and 72.8% have stability < 0.5 . Figure 5 illustrates the edge-stability distribution and mean influence by stability. This supports using epistemic uncertainty as a rejection criterion [Zhu et al., 2025]: a *core* tier ($\tau = 1$) and an *exploratory* tier ($\tau \geq 0.5$) let the majority of edges be flagged as uncertain unless the user opts into the exploratory set.

Table 4: Uncertainty analyses summary ($B = 3$, $n = 20$ prompts).

Analysis	Summary
Rejection	2.5% stab.= 1 (625 edges); 73% stab. < 0.5 .
Alternatives	6.2k contingent edges, 45% influence.
Approx. intervention	Spearman 0.29; effect \uparrow with stability.
Ablation ($n=20$)	16/20 vs. matched; 6.0 [2.7, 9.2], $p=0.012$.
Patching ($n=20$)	17/20 vs. matched; 12.6 [6.8, 17.6], $p=0.0004$.
Prompt-level	Spearman(IR, prob) 0.69 [0.28, 0.89].
CI width (mean IR)	Consensus 0.074; single 0.103.
Sensitivity	$B=2, 3$: 625, IR 0.78; alt. triple: 887, IR 0.79.

Alternatives (value of disagreement). Edges with stability in (1/3, 2/3) but high per-edge influence represent *alternative pathways*. In the same run, 6,214 such alternative edges carry 45% of the total influence of all present edges. Disagreement across configs is thus substantively important: low-agreement edges are not mere noise and can be reported as a second subgraph for users who want to inspect disputed but influential structure.

Variance and bootstrap CI. Over 20 prompts, the standard deviation of consensus IR across prompts (0.054) was higher than the mean std of single-config IR in this run. We report bootstrap 95% CIs for the mean IR across prompts (not prediction intervals). Table 4 summarizes these analyses.

Approximate intervention (internal consistency). We pre-register Spearman(stability, ablation effect) as the success metric for graph-level ablation: zero one edge, recompute influence; effect = drop in total influence Φ . In this run we obtain Spearman = 0.29; mean ablation effect increases with stability band (2/3 configs: $\sim 6.2e-6$, $n = 284$; 3/3 configs: $\sim 1.1e-4$, $n = 116$). The moderate correlation is expected with only three stability levels and supports internal consistency. **Counterfac-**

tual ablation (graph-level): we form two same-size edge sets—top- k by influence among high- vs. low-stability edges—zero each set in turn and measure Δ ; $\Delta_{\text{high}} \geq \Delta_{\text{low}}$ supports that high-stability edges account for more flow. We report Δ_{high} and Δ_{low} in the supplement.

Activation-level intervention. Under the design in Section 4, over $n = 20$ prompts mean recovery is 19.4 ± 10.9 (consensus) vs. 6.8 ± 7.9 (random) vs. 1.6 ± 7.5 (matched); consensus $>$ control in 18/20 and $>$ matched in 17/20. Paired mean(consensus – control) = 12.6 [95% CI: 6.8, 17.6], sign test $p = 0.0004$; paired mean(consensus – matched) = 17.8 [10.8, 23.1], $p = 0.0026$. Sanity: oracle 22.2, uncorrupted 5.0. Figure 2 shows per-prompt recovery. **Ablation** ($n = 20$): mean Δ_{logit} 22.2 ± 6.5 (consensus) vs. 20.1 ± 6.5 (random) vs. 16.1 ± 9.2 (matched); consensus $>$ matched in 16/20 (paired diff 6.0 [2.7, 9.2], $p = 0.012$). Patching gives stronger separation than ablation; both support that consensus positions causally support the clean prediction. We follow Zhang and Nanda [2024], Wang et al. [2024]; alternative corruptions in Appendix G.

Prompt-level. Spearman(consensus IR, target logit prob) = 0.69 [0.28, 0.89] ($n = 20$): when consensus explains more flow, target probability tends to be higher. We interpret this as an exploratory signal, not causal validation. Intervention with subset-of-edges (replacement-model masking) remains future work.

Robustness and multi-prompt. Consensus IR (0.78) exceeds the union-then-influence-pruned-to- $|C_1|$ baseline (0.73) at the same edge budget. Over 20 prompts, consensus IR has mean 0.83, std 0.05, min 0.77—worst-case remains high (min 0.765 in this run).

Stability-weighted selection. At fixed edge budget $k = 625$, consensus ($\tau = 1$) attains IR 0.78 vs. top- k by influence 0.73; threshold-robust consensus beats same-size influence ranking. Top- k by stability \times influence *wins* at smaller budgets: at $k = 200$ (IR 0.64 vs. 0.63 by influence) and $k = 400$ (0.71 vs. 0.67). Over 5 prompts, worst-case IR is higher for top-625 by stab. \times influence (0.71) than for top-625 by influence (0.67), so the stability-weighted variant improves robustness when threshold or prompt

varies. At $k = 625$ and $k = 1,250$, the two strategies are similar (0.73 vs. 0.73, 0.79 vs. 0.79). At large k (e.g. 2,500), top- k by influence slightly leads (0.86 vs. 0.84), so stab. \times influence is most useful at small-to-medium budgets and for worst-case robustness.

Circuit-disagreement taxonomy. Using the core/contingent/noise tiers from Section 3.3: *core* (stability = 1), *contingent* (medium stability, high marginal influence), *noise* (low stability, low influence). In this run, core 625 edges (47.2% of present influence), contingent 6,214 (45.2%); noise 0. Contingent edges appear in 1 or 2 configs (2,497 and 3,717), illustrating config-specific pathways. Top contingent edges by influence appear in configs 2 and 3 only (or 1 only); we interpret them as alternative routes for the target prediction (see supplement for edge list).

View diversity. Pairwise Jaccard between the three configs: edge set 0.025–0.27 (mean 0.13), node set 0.16–0.56 (mean 0.34). Low overlap underscores that consensus is informative despite high view disagreement.

A case study comparing consensus vs. contingent paths is in Appendix F.

Sensitivity. For $B = 2$ (the two stricter configs) and $B = 3$, consensus size and IR are unchanged (625 edges, IR 0.78), since the intersection of the two stricter configs equals the three-config consensus. An alternative threshold triple (0.65, 0.94), (0.82, 0.97), (0.92, 0.995) yields 887 edges and IR 0.79. Full tables are in the supplement.

6 Discussion and Limitations

Uncertainty framing. We quantify uncertainty in circuit discovery by treating multiple graphs as an ensemble and reporting stability and consensus (Section 3.3). The *core* consensus ($\tau = 1$) and the exploratory tier ($\tau < 1$) or full boosted circuit support different use cases. Low-stability, high-influence edges can be reported as alternative pathways. Stability measures agreement across configs, not causal correctness (Section 3.3).

Limitations. (1) *Faithfulness:* We use influence retained [Ameisen et al., 2025] for within-method comparison and activation patching [Zhang

and Nanda, 2024] for causal validation; replacement-model masking is not yet implemented. (2) *Boosting size*: Full $C_1 \cup C_2$ can be large; we provide compact and post-pruned options. When a single threshold is fixed by domain, a single-run graph may suffice; our method is most useful when threshold choice is uncertain. **Future work**: intervention-based faithfulness when supported by the library; multi-CLT alignment (bagging over multiple transcoder checkpoints); bootstrap CIs for per-edge stability; stacking different pruning strategies.

7 Conclusion

We introduced CIRCUS (bagged attribution graphs) to quantify structural uncertainty in mechanistic circuit discovery from arbitrary analyst choices such as pruning thresholds and feature dictionaries. Consensus circuits are $\sim 40\times$ smaller than the union at comparable IR and outperform the same-edge-budget baseline; activation patching confirms that consensus positions causally support predictions ($p = 0.0004$). The taxonomy of core, contingent, and noise edges makes disagreement actionable. The pipeline reuses existing attributions and adds negligible cost. Future work includes replacement-model masking, multi-CLT alignment, and bootstrap CIs for per-edge stability. Code and replication instructions are in the supplement.

Generative AI. Generative AI was used for programming support, editing, and polishing of the manuscript. The author reviewed and takes full responsibility for the content.

Acknowledgements

The author thanks the teams that open-sourced attribution tools and public transcoder checkpoints.

References

Chirag Agarwal, Nari Johnson, Martin Pawelczyk, Satyapriya Krishna, Eshika Saxena, Marinka Zitnik, and Himabindu Lakkaraju. Rethinking stability for attribution-based explanations. In *Inter-*

national Conference on Learning Representations (ICLR), 2022.

Emmanuel Ameisen, Jack Lindsey, et al. Circuit tracing: Revealing computational graphs in language models. <https://transformer-circuits.pub/2025/attribution-graphs/methods.html>, 2025. Anthropic.

Florian Bley, Sebastian Lapuschkin, Wojciech Samek, and Grégoire Montavon. Explaining predictive uncertainty by exposing second-order effects. *Pattern Recognition*, 2024.

Finale Doshi-Velez and Been Kim. Towards a rigorous science of interpretable machine learning. 2017.

Siddharth Gadgil et al. Ensembling sparse autoencoders. 2025.

Gemma Team et al. Gemma 2: Improving open language models at a practical size. 2024.

Prashnna K. Gyawali, Xiaoxia Liu, James Zou, and Zihuai He. Ensembling improves stability and power of feature selection for deep learning models. In *Proceedings of Machine Learning Research (MLCB)*, volume 200, pages 33–45, 2022.

Michael Hanna, Mateusz Piotrowski, Jack Lindsey, and Emmanuel Ameisen. circuit-tracer. <https://github.com/safety-research/circuit-tracer>, 2025.

Anatoly A. Krasnovsky. Measuring uncertainty in transformer circuits with effective information consistency. 2025.

Yaman Kumar, Swapnil Parekh, Somesh Singh, Junyi Jessy Li, Rajiv Ratn Shah, and Changyou Chen. Automatic essay scoring systems are both overstable and oversensitive: Explaining why and proposing defenses. *Dialogue & Discourse*, 14(1): 1–31, 2023.

Jack Lindsey, Emmanuel Ameisen, et al. Circuit tracing: Biology. <https://transformer-circuits.pub/2025/attribution-graphs/biology.html>, 2025. Anthropic.

- Nicolai Meinshausen and Peter Bühlmann. Stability selection. *Journal of the Royal Statistical Society: Series B (Statistical Methodology)*, 72(4):417–473, 2010.
- Meta AI et al. The Llama 3 herd of models. 2024.
- Chris Olah. Mechanistic interpretability, variables, and the importance of interpretable bases. <https://transformer-circuits.pub/2022/mech-interp-essay/index.html>, 2022. Transformer Circuits Thread.
- Joseph Paillard, Angel Reyero Lobo, Denis A. Engemann, and Bertrand Thirion. Aggregate models, not explanations: Improving feature importance estimation. 2026.
- Swapnil Parekh, Yaman Kumar Singla, Changyou Chen, Junyi Jessy Li, and Rajiv Ratn Shah. My teacher thinks the world is flat! interpreting automatic essay scoring mechanism. 2020.
- Daking Rai, Yilun Zhou, Shi Feng, Abulhair Saparov, and Ziyu Yao. A practical review of mechanistic interpretability for transformer-based language models. 2024.
- Lee Sharkey, Bilal Chughtai, Joshua Batson, Jack Lindsey, et al. Open problems in mechanistic interpretability. 2025.
- Yaman Kumar Singla, Swapnil Parekh, Somesh Singh, Changyou Chen, Balaji Krishnamurthy, and Rajiv Ratn Shah. MINIMAL: Mining models for universal adversarial triggers. In *Proceedings of the AAAI Conference on Artificial Intelligence*, volume 36, pages 10587–10595, 2022.
- Kevin Wang et al. Interpretability in the wild: Activation patching and best practices. <https://www.anthropic.com/research/interpretability-in-the-wild>, 2024. Anthropic; activation patching methodology and pitfalls.
- Fred Zhang and Neel Nanda. Towards best practices of activation patching in language models: Metrics and methods. In *International Conference on Learning Representations (ICLR)*, 2024.
- Chenrui Zhu, Louenas Bounia, Vu-Linh Nguyen, Sébastien Destercke, and Arthur Hoarau. Robust explanations through uncertainty decomposition: A path to trustworthier AI. 2025.

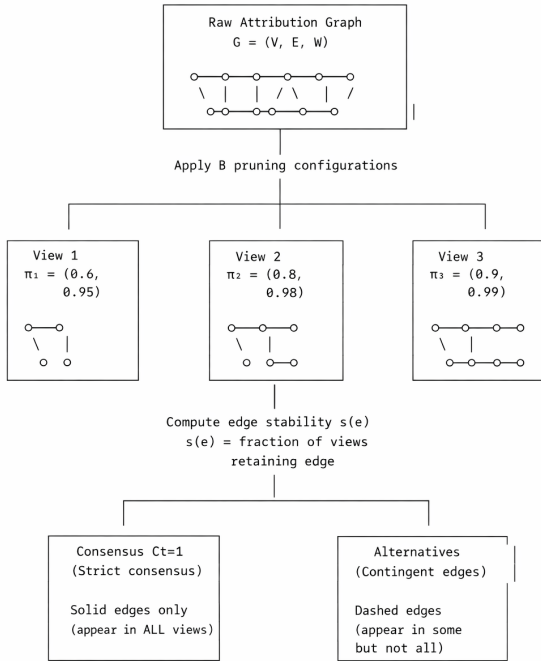


Figure 1: **Bagged attribution pipeline.** One raw attribution graph is pruned under B configurations to yield multiple views; edges receive stability scores $s(e)$. Strict consensus $C_{\tau=1}$ keeps only edges present in all views (solid); dashed edges indicate contingent alternatives. Boosting and causal validation (activation patching) are in Section 3.4 and Section 5.4 (Fig. 2).

Activation patching recovery (hook_site=resid_post, corruption=zero_random)

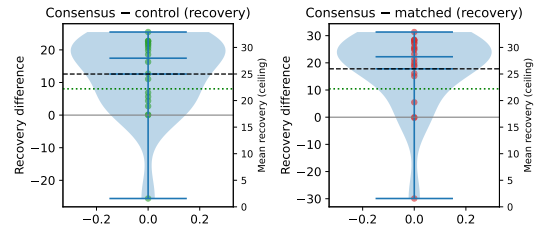


Figure 2: Activation patching recovery ($n = 20$ prompts). Per-prompt recovery difference (patched – corrupted logit): **left** consensus – random control; **right** consensus – matched baseline. Consensus outperforms both baselines (18/20 and 17/20 prompts). Mean paired difference (95% CI): 12.6 [6.8, 17.6] vs. control; 17.8 [10.8, 23.1] vs. matched. The horizontal line marks oracle recovery (ceiling).

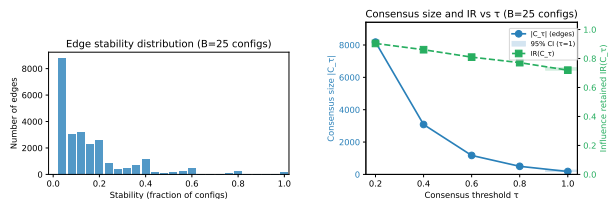


Figure 3: Stability with $B = 25$ configs. **Left:** Edge stability histogram. **Right:** Consensus size $|C_{\tau}|$ and $IR(C_{\tau})$ vs. τ (elbow curve); shaded bands at strict consensus ($\tau = 1$) show bootstrap 95% CI over configs.

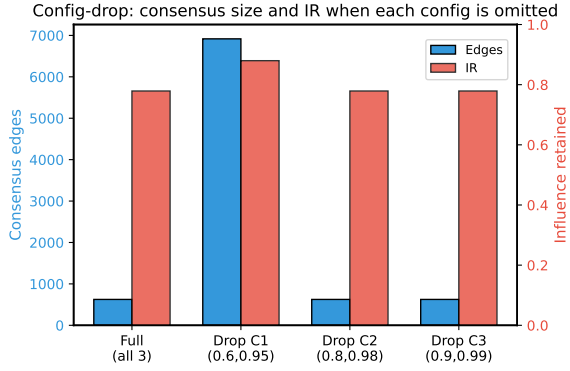


Figure 4: Config-drop (leave-one-config-out): consensus edge count and influence retained when each pruning config is omitted. Dropping the loosest config changes consensus substantially; dropping a stricter config does not.

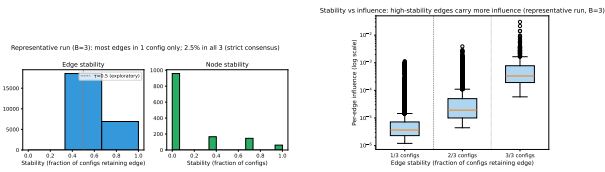


Figure 5: Stability vs. influence. **X-axis:** edge stability $s(e)$. **Left Y-axis:** count of edges (histogram). **Right Y-axis:** mean influence per edge (line with error bars). High-stability edges are rare but carry the most influence, supporting threshold-robust consensus as the primary circuit.

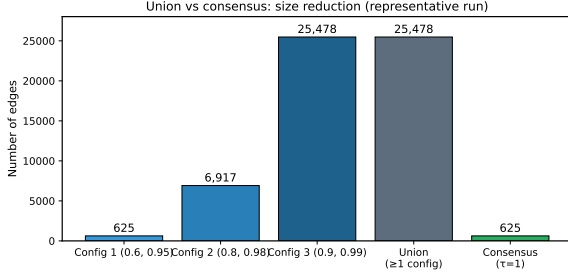


Figure 6: Union vs. consensus: edge count per graph (representative run). Consensus is a $\sim 40\times$ smaller subset with comparable influence retained (Table 2).

A Uncertainty analyses summary table

Table 4 in Section 5.4 summarizes rejection criteria, alternatives, Spearman correlations, 95% CIs for mean IR, activation patching results, and sensitivity.

B Union vs. consensus: edge-count figure

C Pipeline and Architecture

Figure 1 and the pipeline overview in Section 3 (after the figure) define inputs, outputs, and deliverables. Appendix D gives the algorithms.

D Algorithms

Algorithm 1: Stability and consensus from B views.

- **Input:** Full attribution graph $\mathcal{G} = (V, E, W)$; B pruning configurations $\{\pi_b\}_{b=1}^B$; consensus threshold $\tau \in [0, 1]$.
- **Output:** Per-edge stability $s(e)$ for $e \in E$; consensus edge set $C_\tau = \{e : s(e) \geq \tau\}$; union $E^{\text{union}} = \bigcup_b E^{(b)}$.

- **Steps:** (1) For each $b \in [B]$, obtain pruned edge set $E^{(b)}$ by applying π_b to \mathcal{G} . (2) For each $e \in E^{\text{union}}$, set $s(e) = \frac{1}{B} \sum_{b=1}^B \mathbb{1}[e \in E^{(b)}]$ (Eq. 1). (3) Set $C_\tau = \{e : s(e) \geq \tau\}$ (Eq. 2). (4) Optionally compute $\text{IR}(C_\tau)$ and $\text{IR}(E^{\text{union}})$ via Eq. 3.

Algorithm 2: Boosting (residual round).

- **Input:** Full graph \mathcal{G} ; consensus circuit C_1 (e.g., C_τ from Algorithm 1 with $\tau = 1$); residual fraction $\alpha \in (0, 1]$ (e.g., top 90% of residual).
- **Output:** Residual edge set C_2 ; boosted circuit $C_1 \cup C_2$; $\text{IR}(C_1)$, $\text{IR}(C_2)$, $\text{IR}(C_1 \cup C_2)$.
- **Steps:** (1) Build residual graph by zeroing weights for edges in C_1 ; compute per-edge influence on this residual graph. (2) Let C_2 be the set of edges that capture fraction α of the residual influence (e.g., greedy by decreasing residual influence until cumulative residual reaches α). (3) Set boosted circuit to $C_1 \cup C_2$. (4) Compute $\text{IR}(C_1)$, $\text{IR}(C_2)$, $\text{IR}(C_1 \cup C_2)$ via Eq. 3.

E Additional threshold-sweep results ($B = 25$, config-drop)

With a grid of $B = 25$ pruning configs (same attribution, 5×5 node/edge threshold grid), the edge stability distribution is rich: stability takes many values in $[0, 1]$ rather than $\{1/3, 2/3, 1\}$. Consensus size $|C_\tau|$ and $\text{IR}(C_\tau)$ decrease as τ increases (e.g., $\tau = 0.2$: 8,178 edges, IR 0.90; $\tau = 0.5$: 1,588 edges, IR 0.82; $\tau = 1$: 180 edges, IR 0.72). Bootstrap over configs (100 samples) yields 95% CI for $|C_1|$ [180, 265] and for $\text{IR}(C_1)$ [0.72, 0.74]. Figure 3 and Figure 4 in Section 5.1 show the elbow plot and config-drop analysis. Dropping the loosest config (0.6, 0.95) yields a two-config consensus of 6,917 edges (IR 0.88); the full three-config consensus remains 625 edges (IR 0.78). Dropping either of the stricter configs leaves consensus unchanged.

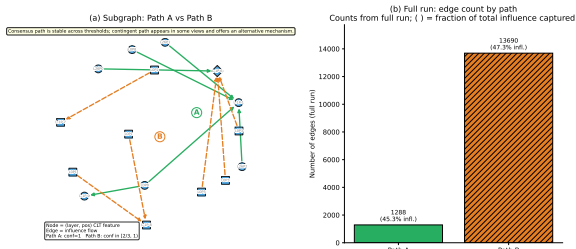


Figure 7: Case study: two short paths (6–12 nodes). Nodes are (layer, position) CLT features; edges show influence flow. Solid edges = consensus path (all configs); dashed = contingent path (subset of configs). Full subgraph in supplement.

F Case study: consensus vs. contingent paths

We illustrate two pathways on a representative prompt: edges in all configs (consensus path) vs. edges in a subset of configs (contingent path). Figure 7 shows a minimal subgraph: solid edges appear in every pruning config; dashed edges appear in one or two configs and carry non-negligible influence. The contingent path can be interpreted as an alternative mechanism for the same prediction; including it supports the value of reporting contingent edges alongside the core.

G Activation patching: alternative corruption (swap across prompts)

We replicate the activation patching experiment with an alternative corruption: swapping activations across prompts. For each prompt i , the clean run is on prompt i ; the corrupted run uses the same prompt but with 50% of (layer, pos) slots replaced by activations from prompt $(i + 1) \bmod n$. We then patch back k slots from the clean run and measure recovery = patched logit – corrupted logit for the clean target token. Over $n = 20$ prompts, we report paired-mean bootstrap 95% CI and sign test. Mean recovery is

See supplement for reproduction.

Figure 8: Swap-prompt corruption ($n = 20$): per-prompt recovery difference (consensus – control, consensus – matched). Heterogeneity across prompts motivates reporting both mean CI and sign test.

7.34 ± 10.05 (consensus) vs. 3.48 ± 4.96 (random control) vs. 0.43 ± 0.86 (matched). Consensus > control in 12/20 and consensus > matched in 13/20. Paired mean(consensus – control) = 3.86 [95% CI: 1.31, 7.11], sign test $p = 0.50$; paired mean(consensus – matched) = 6.91 [2.87, 11.42], $p = 0.26$. The mean improvement is positive (CI excludes zero for consensus – matched) but the median paired difference is weaker, hence the large sign-test p -values; effect sizes are smaller than under zero-random corruption. Figure 8 shows per-prompt recovery.